MBE Advance Access published March 24, 2012

Resequencing Data Provide No Evidence for a Human Bottleneck in Africa during the Penultimate Glacial Period

Per Sjödin,[1] Agnès E. Sjöstrand,[1,2] Mattias Jakobsson,[1,3] and Michael G.B. Blum[*,4]

[1]Department of Evolutionary Biology, Evolutionary Biology Centre, Uppsala University, Uppsala, Sweden
[2]UMR 7206 Eco-anthropologie et Ethnobiologie, CNRS-MNHN-Université Paris, Paris, France
[3]Science for Life Laboratory, Uppsala University, Uppsala, Sweden
[4]Laboratoire TIMC-IMAG UMR 5525, Centre National de la Recherche Scientifique, Université Joseph Fourier, Grenoble, France

***Corresponding author:** E-mail: michael.blum@imag.fr.

Associate editor: Sohini Ramachandran

Abstract

Based on the accumulation of genetic, climatic, and fossil evidence, a central theory in paleoanthropology stipulates that a demographic bottleneck coincided with the origin of our species *Homo Sapiens*. This theory proposes that anatomically modern humans—which were only present in Africa at the time—experienced a drastic bottleneck during the penultimate glacial age (130–190 kya) when a cold and dry climate prevailed. Two scenarios have been proposed to describe the bottleneck, which involve either a fragmentation of the range occupied by humans or the survival of one small group of humans. Here, we analyze DNA sequence data from 61 nuclear loci sequenced in three African populations using Approximate Bayesian Computation and numerical simulations. In contrast to the bottleneck theory, we show that a simple model without any bottleneck during the penultimate ice age has the greatest statistical support compared with bottleneck models. Although the proposed bottleneck is ancient, occurring at least 130 kya, we can discard the possibility that it did not leave detectable footprints in the DNA sequence data except if the bottleneck involves a less than a 3-fold reduction in population size. Finally, we confirm that a simple model without a bottleneck is able to reproduce the main features of the observed patterns of genetic variation. We conclude that models of Pleistocene refugium for modern human origins now require substantial revision.

Key words: human origins, African genetic diversity, penultimate glacial age, approximate Bayesian computation, African bottleneck, oxygen isotope 6.

Research article

Introduction

Quaternary ice ages have deeply affected the genetic diversity of many living organisms (Hewitt 2000) and humans may be no exception. There is a variety of facts to suggest that humans drastically decreased in number during the Marine Isotope Stage 6 (MIS6) time period, which corresponds to the penultimate major ice age 190–130 kya (Lahr and Foley 1998). The marine isotope stages correspond to the different stages of mass ratio between ^{18}O and ^{16}O stable isotopes found along marine stratigraphic sequences. The mass ratio between ^{18}O and ^{16}O being proportional to the temperature at which the sediments were formed, these stages correspond either to glacial periods or interglacial periods (Shackleton et al. 1977). MIS6 had very similar conditions to the last ice age (MIS2), though it was a little colder (Petit et al. 1999) and the ice sheets extended over a slightly greater area than during MIS2 (Hetherington and Reid 2010). During MIS6, deserts, savanna, and open dry forest widened, whereas rain forest receded (Van Andel and Tzedakis 1996; Dupont et al. 2000), resulting in open grassland that would not protect early humans against predators (Lahr and Foley 1998).

There are several lines of genetic evidence for a bottleneck: All present-day mitochondrial sequences coalesced into a single individual—the "mitochondrial Eve"—at the onset of MIS6 (Gonder et al. 2007; Behar et al. 2008); numerical simulations tuned to reproduce autosomal genetic diversity also point to a bottleneck during MIS6 with a human effective population size smaller than 2,000 individuals at the bottleneck's inception (Fagundes et al. 2007); a bottleneck during MIS6 can account for the 8-fold difference between the times to the most recent common ancestor of mitochondrial and autosomal genes (Blum and Jakobsson 2011); and the 1.5–4 times lower level of genetic diversity in humans compared with great apes can been attributed to a bottleneck (Kaessmann et al. 2001). Finally, the timing of the bottleneck is consistent with the available evidence on the morphological evolution of humans, which indicates that the first known specimen of *Homo sapiens* emerged during or just before MIS6 (White et al. 2003; McDougall et al. 2005). Because there is a temporal match between the evidence for the first specimen of *H. sapiens* and the MIS6 bottleneck, which would have promoted population differentiation, some authors refer to the MIS6 bottleneck as a "speciation" bottleneck (Garrigan and Hammer 2006; Fagundes et al. 2007).

Two scenarios have been proposed for how the climate change during MIS6 affected the human population (Lahr and Foley 1998). In the "fragmentation" hypothesis (see fig. 1), the human population in Africa would have been divided into several geographically restricted groups or refugia with no gene flow between them. Extensive aridity in Africa during MIS6, far more severe than during the Last Glacial Maximum (Castañeda et al. 2009), would have

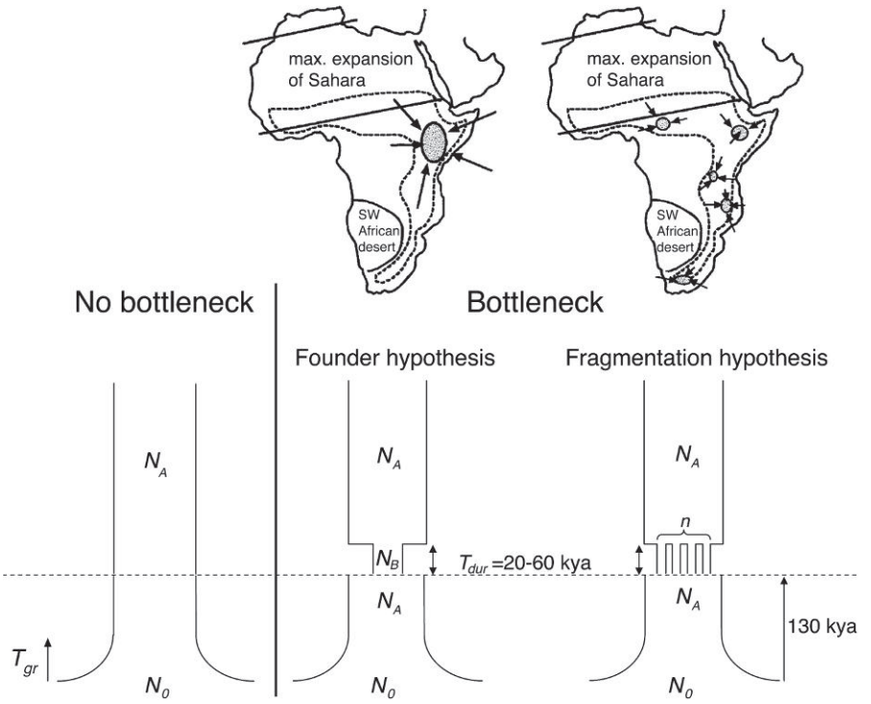

FIG. 1. Schematic overview of the three investigated demographic models. The end of MIS6, approximately 130,000 kya, is marked by a dashed line. The map of Africa where potential human refugia are displayed has been excerpted from Lahr and Foley (1998). We denote by N_A and N_B the effective population sizes before and during the bottleneck, by N_0 the present-day effective population size, and by n the number of subpopulations during the bottleneck.

caused the contraction and fragmentation of available areas that could sustain humans. The alternative "founder" hypothesis postulates that of all the hominid populations living in Sub-Saharan Africa, only one is ancestral to modern humans. Candidates for a refuge during the long cold MIS6 are the south coast of South Africa with its unusual confluence of plant diversity, coastline richness, and moderate climate (Marean et al. 2007; Marean 2010) as well as East Africa where the earliest well-dated anatomically modern humans have been described (McDougall et al. 2005).

Compared with non-African populations, African populations are good candidates for detecting a potential bottleneck 130 kya because non-African populations have been through a more recent out-of-Africa bottleneck, which masks patterns of earlier bottlenecks (Voight et al. 2005; Amos and Hoffman 2009). Furthermore, the San and the Biaka Pygmy carry paternal and maternal lineages belonging to some of the deepest clades known among modern humans and may therefore carry important information for reconstructing ancient human demography (Knight et al. 2003; Behar et al. 2008; Henn et al. 2011).

In this study, we search for evidence of a bottleneck during MIS6 using sequence data from 61 autosomal 20 kb DNA fragments typed in the African Biaka, Mandenka, and San populations (Wall et al. 2008; Hammer et al. 2010). We investigate three different demographic models: a model without a bottleneck, a model with a bottleneck at MIS6, and a model where the human population was fragmented during MIS6.

Materials and Methods

We summarized the information contained in the sequence data using summary statistics that are informative with respect to ancient demography (table 1; Depaulis et al. 2003; Voight et al. 2005). The summary statistics were computed for each of the 61 autosomal sequences (supplementary tables 1–3, Supplementary Material online) and the means and variances were retained (table 1). We evaluated the statistical support of a bottleneck during MIS6 using Approximate Bayesian Computation (ABC; Beaumont et al. 2002; Csilléry et al. 2010). The ABC approach relies on comparing the observed values of the summary statistics to summary statistics simulated under the two versions of the bottleneck model (fragmentation and founder) as well as under a "no bottleneck" hypothesis that does not include any bottleneck during MIS6 (fig. 1). The choice of mutation rate can impact the results and because there is a 2–3-fold difference between the mutation rate estimated from mother–father–child trios (or quartet; $\sim 10^{-8}$/bp/generation; Roach et al. 2010; The 1000 Genomes Project Consortium 2010) and the mutation rate derived from human–chimp comparisons ($\sim 2.5 \times 10^{-8}$/bp/generation; Nachman and Crowell 2000; Fagundes et al. 2007; Gutenkunst et al. 2009; Laval et al. 2010), we considered both estimates of the mutation rate in our analyses.

Sequence Data

The data comprise 61 resequenced independent intergenic regions from the autosomes, which are in areas of medium

Table 1. Summary Statistics Computed for 61 Autosomal Sequences.

	$\bar{S}$	$\bar{D}$	$\bar{D}^*$	$\bar{H}$	$\bar{C}$	Var *S*	Var *D*	Var D^*	Var *H*
San	23.98	−0.23	−0.14	0.58	213.62	50.28	0.49	0.88	6.39
Biaka	28.1	−0.32	−0.23	0.02	199.62	102.26	0.35	0.7	13.51
Mandenka	27.62	−0.26	−0.23	−0.31	190.51	89.61	0.26	0.66	17.51
Pooled sample	43.51	−0.77	−0.99	−0.23	139.30	122.55	0.24	0.63	14.38

NOTE.—The summary statistics are the number of SNPs *S*, Tajima's *D*, Fu and Li's D^*, Fay and Wu's *H*, and Hudson's estimate of the recombination rate *C* (Thornton 2003). We summarized the 61 values of the summary statistics using the mean and the variance (except for Hudson's *C* for which we computed only the mean).

or high recombination at least 100 kb from the nearest gene, and the sequence data were generated by Wall et al. (2008) and Hammer et al. (2010). The sequenced regions were chosen to minimize any potential confounding effects of natural selection (Wall et al. 2008). Each region encompasses ~20 kb and generally consists of three 2 kb sequence fragments, separated by 7 kb of unsequenced DNA. We considered three African populations: Mandenka (16 sampled individuals), Biaka (15 sampled individuals), and San (9 sampled individuals) from Namibia. The sequences of two common chimpanzees, available in the database, were used as outgroups.

Statistical Analysis

For each population, we used ABC to find the range of demographic parameters that yield summary statistics similar to the empirical summary statistics computed for the three populations. We chose to use the following summary statistics: mean and variance over the 61 loci of the number of single nucleotide polymorphisms (SNPs), mean and variance of Tajimas's *D*, mean and variance of Fu and Li's D^*, mean and variance of Fay and Wu's *H*, and mean of Hudson's estimate of the recombination rate (Hudson 1987). Although phased haplotypes are provided in the database, we do not consider haplotypic summary statistics since these are known to be sensitive to recent admixture (Lohmueller et al. 2010). For each scenario of human demographic history, we simulated 100, 000 multilocus summary statistics as follows.

- Generate the demographic parameters according to the prior distributions given in table 2.
- For each of the 61 loci, generate a sample using the software *ms* (Hudson 2002). The *ms* software is based on the coalescent framework; it first generates a random genealogy of the sample under a particular demographic model and mutations are thereafter randomly placed on the genealogy. For each set of demographic parameters, we generated 61 autosomal sequence regions with the same sample sizes and the same sequence lengths as in the empirical data (see supplementary tables S1–S3, Supplementary Material online).
- Compute the summary statistics, using the "libsequence" C++ library (Thornton 2003) for the simulated sequences in order to obtain the (Euclidean) distance between observed and simulated summary statistics. Before computing the distances, standardize the summary statistics so that they have a variance equal to 1.

When performing parameter inference, we retained the half percent of the simulations (500 out of 100,000 simulations) with the shortest distances between simulated and observed statistics. After this rejection step, we used heteroscedastic regression adjustment to account for the difference between simulated and observed summary statistics (Blum and François 2010). The adjustment step reduces the variance of the accepted parameter values, which is typically inflated compared with an ideal sample based on exact matches (i.e., null distances; Csilléry et al. 2010).

To perform model selection, we simulated 100,000 data sets for each of the three models and computed the three posterior probabilities with two different methods. In the first method, we retained the half percent of the 300,000 simulations with the shortest distances and assumed that the proportions of accepted simulations in each model are proportional to the posterior probabilities (Pritchard

Table 2. Prior Distributions for Demographic Parameters.

	Scenario			Values		
Parameter	**1**	**2**	**3**	**Min.**	**Max.**	**Distribution**
Ancestral effective population size N_A	•	•	•	5,000	35,000	Uniform
***d*, where $N_0 = N_A 10^d$**	•	•	•	0	1.5	Uniform
Present effective population size N_0	•	•	•	5,000	1,106,797	$N_A \cdot 10^d$
***b*, where $N_B = N_A 10^b$**		•	•	−1.5	0	Uniform
Effective population size during bottleneck N_B		•	•	158	35,000	$N_A \cdot 10^b$
Number of subpopulations in bottleneck *n*			•	2	10	Integer uniform
Start time for expansion phase T_{gr}	•	•	•	0	100,000	Uniform
Duration of bottleneck T_{dur}		•	•	20,000	60,000	Uniform
Start time for bottleneck phase T_b		•	•	150,000	190,000	130,000 + T_{dur}

NOTE.—Scenarios 1–3 correspond to the (1) no bottleneck model, (2) founder model, and (3) fragmentation model.

Table 3. Posterior Probabilities of the Different Demographic Models Based on 61 Autosomal Sequences.

	High mutation rate			Low mutation rate		
	San	Biaka	Mandenka	San	Biaka	Mandenka
No bottleneck	**0.79**	**0.84**	**0.81**	**0.91**	**0.88**	**0.87**
Founder bottleneck	**0.06**	**0.04**	**0.07**	**0.07**	**0.06**	**0.04**
Fragmented bottleneck	**0.15**	**0.12**	**0.12**	**0.02**	**0.06**	**0.09**

NOTE.—Estimates were obtained using multinomial logistic regression (Beaumont 2008).

et al. 1999). The second—more sophisticated—method fits a multinomial logistic regression $\Pr(Y|s)$ between the summary statistics s and a trichotomous variable $Y \in \{1, 2, 3\}$ that corresponds to the model index. Inserting the values of the observed summary statistics s_{obs} into the regression equations gives the posterior probabilities $\Pr(Y = i|s_{obs})$, $i = 1, 2, 3$, for the three models (Beaumont 2008).

We checked for population structure (Pritchard et al. 2000) within each population because the three investigated demographic models assume homogenous populations, but we found no indication of stratification.

To assess if there is enough information in the genetic data to distinguish between the three models, we considered a leave-one-out method. For each model (no bottleneck, founder, or fragmentation), we repeated 5, 000 times the following procedure: i) pick the simulated genetic data from a particular simulation among the 100, 000 simulations of the corresponding model, ii) use the summary statistics of the chosen simulation as target instead of the empirical data, and iii) estimate the model probabilities using the remaining 299,999 simulations. Using the method based on multinomial logistic regression, we assign each of the 3× 5,000 simulated cases to the model with the greatest posterior probability. All ABC analyses were performed using the R *abc* package (Csilléry et al. 2012).

We set the prior distribution of the demographic parameters (table 2) so that the bottleneck ended 130 kya and started at a time uniformly distributed between 150 and 190 kya. In all three demographic models, we assumed that Sub-Saharan African populations experienced demographic expansion (Voight et al. 2005; Cox et al. 2009). For the mutation rate, we chose two different priors, each accounting for the variability of mutation rates across loci. For the first prior, we estimated a mutation rate for each of the 61 markers by computing the mean number of nucleotide differences between two chimp sequences and the human sequences. We assumed a genetic divergence of 6 myr between human and chimpanzee and a generation time of 25 years. We then fit a Gamma distribution to the 61 estimated mutation rates. In units of generations, we obtained a Gamma distribution with a shape parameter of 17.86 and a scale parameter of 1.62×10^{-9} (mean $= 2.9 \times 10^{-8}$ mutations/bp/generation). For the second prior, we chose a Gamma distribution parameterized so that the mean mutation rate corresponded to 1.10×10^{-8}/bp/generation (The 1000 Genomes Project Consortium 2010) and the variance is the same as in the first prior. We further assumed a Gaussian distribution, with mean f_{mean} and variance f_{var}, for the ratio f of effective recombination rate to effective mutation rate (Plagnol and Wall 2006). The prior for f_{mean} and f_{var} were uniform between 0.2 and 2.0 and between 0 and 1.0, respectively. Recombination rates were assumed to be constant within loci but to vary across loci.

Results

We first evaluated the relative statistical support of the founder, the fragmentation, and the no bottleneck models. For each of the three African populations and both mutation rates, we find that the no bottleneck model has the highest posterior probability (table 3 and supplementary table 4, Supplementary Material online). When using multinomial logistic regression to evaluate posterior probabilities, the probability of the model without a bottleneck is at least 79% for each African population.

The potential bottleneck that we investigate is ancient, occurring more than 130 kya, and it is therefore uncertain if there is enough information in the sequence data to distinguish between the demographic models. The out-of-Africa and the out-of-Beringia bottlenecks left detectable signals in human genetic diversity, but they occurred much more recently than MIS6 (Voight et al. 2005; Amos and Hoffman 2009). We consider three potential lines of evidence to assert that there is sufficient information in the data to discard a bottleneck during MIS6. We define the bottleneck intensity, b, by

$$N_B = N_A \times 10^b, \quad (1)$$

where N_B is the total population size during the bottleneck and N_A denotes the ancestral population size before the bottleneck. A value of $b = -1.5$ corresponds to an extreme bottleneck with a 30-fold reduction of population size, whereas there is no bottleneck when $b = 0$.

First, if MIS6 is too ancient to affect the distribution of genetic variation in modern populations, the expected posterior distribution of model parameters that are related to this period of time should be the same as the prior distribution of these parameters. This is not what we observe. Although the prior distribution for b is uniform between −1.5 and 0, the peak of the posterior distribution is typically very close to $b = 0$ and values of b smaller than −0.5 are unlikely ($P < 8\%$ for each population when averaging over models and mutation rates; fig. 2 and supplementary figure 1, Supplementary Material online). Second, we investigated whether the correct model was inferred when the genetic data were simulated from that particular model. For a severe bottleneck, a detectable signal is still present in the sequence data: When $b = -1.5$, we correctly assign 97%

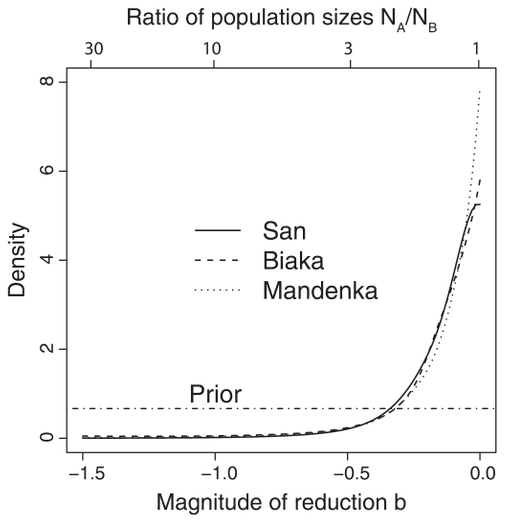

FIG. 2. Posterior distributions of the intensity b of the bottleneck after averaging over bottleneck models (the founder and fragmentation models) and mutations rates. The population size N_B during the bottleneck is given by $N_B = N_A \times 10^b$, where N_A is the population size before the bottleneck. There is a 30-fold reduction of population size when $b = -1.5$, a 3-fold reduction of population size when $b = -0.5$, and no reduction in size when $b = 0$.

of the cases when simulations from the founder model are used as target data, and this number decreases to 79% for the fragmentation model (fig. 3). For a mild bottleneck, a 3-fold reduction of population size ($b = -0.5$), these proportions drop to 32% and 50% for the founder and the fragmentation models. Figure 3 shows that for a bottleneck with $b = -0.5$, 20% of the founder and 38% of the fragmentation simulations are incorrectly assigned to the no bottleneck model. Thus, there is a nonnegligible chance that the model without a bottleneck receives the largest support if the data were generated under a bottleneck model with $b \geqslant -0.5$. Third, for the empirical data, recall that the support for the no bottleneck model was at least 79% for each population and both mutation rates (table 3). For the particular 20% (founder model) and 38% (fragmentation) of the mild-bottleneck simulations ($b = -0.5$) that were incorrectly assigned to the no bottleneck model, we investigated the relative support for the three different models. We found that a strong support $\geqslant 79\%$ for the no bottleneck model occurs in $<1\%$ of these simulations giving evidence that the observed data are also inconsistent with a mild-bottleneck ($b = -0.5$).

To understand where the signal against a bottleneck comes from in the genetic data, we searched for the summary statistics that penalize the bottleneck models. The mean Fay and Wu's $H = 0.58$ of the San sample is large compared with the values simulated by all three demographic models suggesting that there is a deficit of high-frequency mutations compared with intermediate frequency mutations in the San sample (fig. 4). There is a gradient among models, with the founder model generating mean Fay and Wu's H least similar to empirical values, followed by the fragmentation model, and the no bottleneck model generates values that are most similar. For the Biaka and the Mandenka samples, the variance of the Tajima's D over the 61 loci is small (table 1) even when compared with the simulations performed without a bottleneck. A typical footprint of bottleneck is, in fact, an unexpectedly "large" variance of Tajima's D (Haddrill et al. 2005; Voight et al. 2005). Once again, we find a gradient among models: The founder model generates the most different and largest values, the no bottleneck model generates the most similar values, and the fragmentation model is in-between. These are the summary

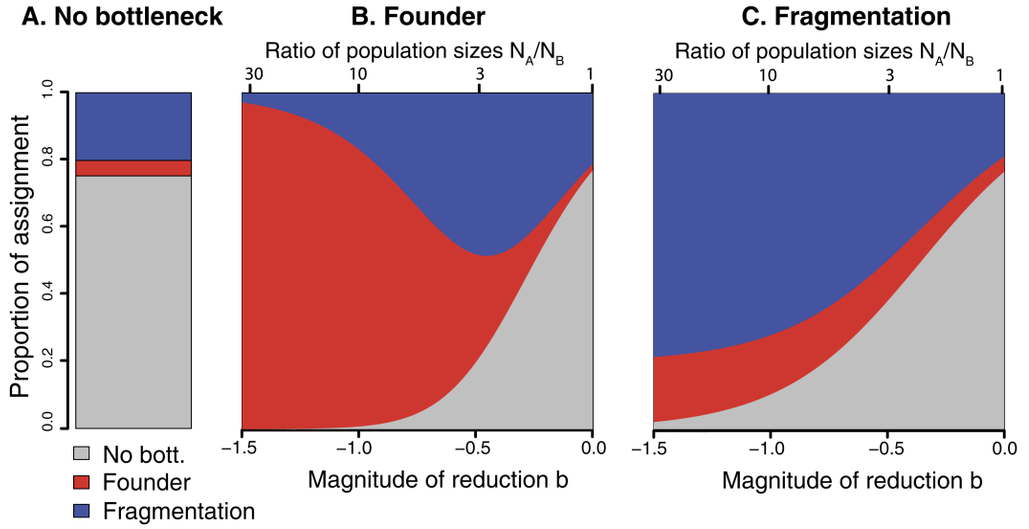

FIG. 3. Proportions of simulated data assigned to each model when simulations were performed under the (*A*) no bottleneck, (*B*) founder, and (*C*) fragmentation model. For each model, we performed model selection using 100, 000 simulations per model. For each model, the proportion of correctly assigned simulations was estimated with a total of 5, 000 simulations that were considered as target data. For the two bottleneck models, we used a smoothing procedure (multinomial logistic regression) to display the proportions of simulations assigned to each model as a function of the bottleneck parameter b.

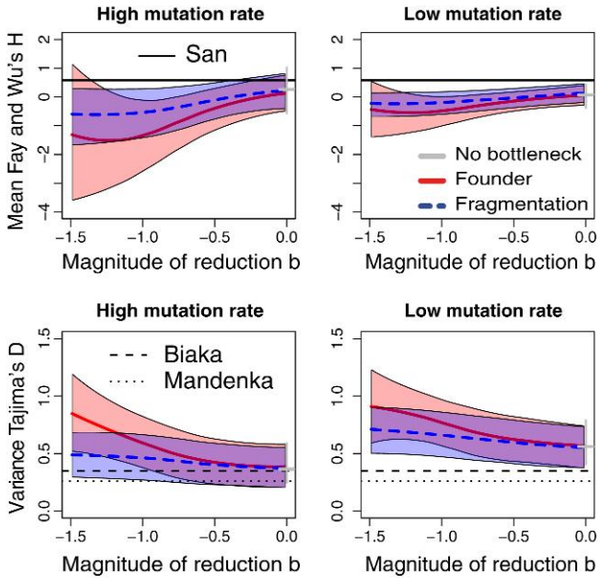

FIG. 4. Expected values of the mean (over 61 loci) Fay and Wu's *H* (upper panels) and Tajima's *D* (lower panels) as functions of the bottleneck intensity. The colored lines represent the expected values and the colored envelopes show the approximate 95% CI estimated from nonlinear regression. Specifically, the CI ranged from $m(b) - 2\sigma_-(b)$ to $m(b) + 2\sigma_+(b)$, where $\sigma_-(b)$ and $\sigma_+(b)$ are nonlinear estimates of the standard deviation of the negative and positive residuals. The plain, dashed, and dotted black horizontal lines correspond to the summary statistics computed for the San, Biaka, and Mandenka samples.

statistics that most clearly distinguish between bottleneck models and a model without a bottleneck, but other summary statistics also add weight to the inference (supplementary fig.s 2 and 3, Supplementary Material online).

We finally tested if the different demographic models, after having been fitted to the three populations, were able to reproduce the observed summary statistics. We simulated 2,000 replicates of the summary statistics using demographic parameters that were drawn from their posterior distribution. Since there are too many summary statistics to easily visualize, we applied principal component analysis to graphically project the posterior distributions of the summary statistics in two dimensions (Cornuet et al. 2010; Berlin et al. 2011). These "posterior predictive checks" show that each demographic model provides a good fit to the summary statistics computed from the empirical data (fig. 5). To explore the match between observed and simulated summary statistics individually, we used two-sided posterior predictive *P* values (Gelman et al. 2003) as an exploratory tool (supplementary table 5, Supplementary Material online). For the model without a bottleneck, most posterior *P* values are found to be larger than 5% for both mutation rates confirming that this simple demographic model provides a good fit to the summary statistics. The exceptions are the variance of the number of SNPs for the San, the mean of the Tajima's *D* for the Biaka, and the variance of the Tajima's *D* for the Mandenka. The models that include a bottleneck do not provide a better fit to these summary statistics for which the posterior *P* values are also smaller than 5% for one of the two mutation rates (see supplementary table 5, Supplementary Material online).

Discussion

Our study shows that autosomal sequence variation from two hunter–gatherer populations (San and Biaka) and one agriculturalist population (Mandenka) do not provide evidence for a bottleneck during the cold period of MIS6. Using an ABC approach, we find that the simple demographic scenario without a bottleneck during MIS6 (the no bottleneck model in fig. 1) is preferred to the alternative models (the founder and fragmentation versions of a bottleneck) for all three populations. Although the three considered models can be almost perfectly fitted to reproduce the observed summary statistics (fig. 5), the fitted bottlenecks involve a less than a 3-fold reduction during MIS6 (fig. 2) making them indistinguishable from the model without a bottleneck. With a less than a 3-fold reduction of population

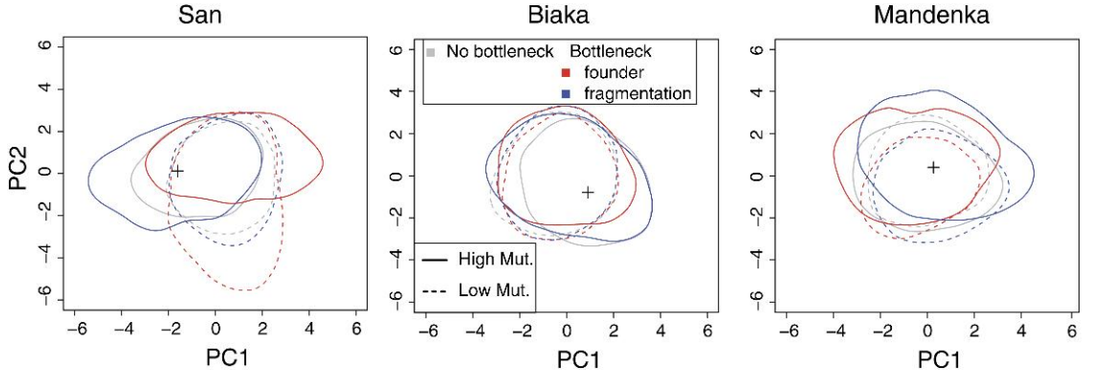

FIG. 5. Posterior predictive checks of the demographic models. To display the joint posterior distribution of the nine summary statistics, we project the posterior simulations into the first two axes resulting from a principal component analysis. Curves correspond to the 95% envelopes of the posterior predictive distributions and crosses correspond to the actual summary statistics. High Mut. stands for high mutation rate and Low Mut. stands for low mutation rate.

size, there is insufficient signal in the summary statistics to clearly discriminate between the demographic models (fig. 3). A reduction in population size by a factor of 3 would still be a noteworthy event, but in comparison with the bottlenecks associated out-of-Africa migration or the peopling of the Americas, it would not stand out as an extraordinary event, and, as we have demonstrated, it would not leave substantial traces in population-genomic patterns of variation. More severe bottlenecks are, however, detectable. Assuming an effective population size of the order of $N = 10,000$ individuals corresponds to autosomal gene genealogies going back, on average, $2 \times 2N = 40,000$ generations. Since the end of MIS6 occurs about 5,000–6,000 generations ago, the bottleneck would have taken place in the most recent quarter of the genealogical tree. Intuitively, a moderate to strong bottleneck occurring during MIS6 would leave a detectable signal in the data because bottlenecks distort the shape of the gene trees (e.g., Galtier et al. 2000).

Pleistocene Refugia Hypothesis

The lack of evidence for a severe human bottleneck during MIS6 suggests a revision of the current Pleistocene refugium model of anatomically modern human origins (Lahr and Foley 1998) and, more generally, has implications for evaluating the importance of ice ages on speciation (Klicka and Zink 1997). Of particular relevance is the "Pleistocene refugia hypothesis" (Haffer 1969). It assumes that during several dry climatic periods of the Pleistocene, the tropical forest was divided into a number of smaller forests that were isolated from each other by tracts of nonforest vegetation and that the remaining forests served as refugia for numerous populations (Haffer 1969). Fragmentation of the African forest is debated, and simulations of paleovegetation during the glacial ages suggest that African tropical forests were not severely displaced by expanding grasslands during glacial ages (Cowling et al. 2008). Nonetheless, the fact that the mitochondrial time since the most recent common ancestor (TMRCA) of many subspecies of orangutans and common chimpanzees overlap with the cold MIS6 has been interpreted as that Pleistocene refugia may have promoted speciation and diversification in the *Hominidae* family (Arora et al. 2010; Bjork et al. 2011). As shown in this study, however, the occurrence of a mitochondrial TMRCA during MIS6 is not sufficient evidence for a severe reduction in population size associated with glacial refugia.

Population Size and Density during the Pleistocene

A small human effective population size, on the order of 10,000 individuals, which is smaller than the effective population size of most great apes, has been interpreted as a result of a very long history, starting $\sim$2 mya, of a small population size, coined as the long-necked bottle model (Harpending et al. 1998; Hawks et al. 2000). Our findings are consistent with this hypothesis, but, depending on the mutation rate, we find either an effective population size of $N_A = 12,000$ (95%CI =9,000–15,500 when averaging over all three demographic models) using the mutation rate calibrated with the human–chimp divergence or an effective population size of $N_A = 32,500$ individuals (95%CI = 27,500–34,500) using the mutation rate given by whole-genome trio analysis (The 1000 Genomes Project Consortium 2010; supplementary fig. 4 and table 6, Supplementary Material online). Not surprisingly, the estimated "effective" mutation rates $\theta = 4N_A\mu$ are comparable for the two mutation rates we considered and are equal to 1.4×10^{-3}/bp/generation (95%CI $= (1.1 - 1.7) \times 10^{-3}$).

Relating the estimated effective population size to the census population size during the Pleistocene is a difficult task because there are many factors affecting the effective population size (Charlesworth 2009). Nevertheless, based on published estimates of the ratio between effective and census population size, a comprehensive value on the order of 10% has been found by Frankham (1995). This 10% rule roughly predicts that 120,000–325,000 individuals (depending on the assumed mutation rate) lived in Sub-Saharan Africa some 130 kya. Assuming that the range of humans extends over all the 24 millions km^2 of Sub-Saharan Africa, the density of humans at that time would have been extremely low between 0.5 and 1.4 individual per 100 km^2, which is even lower than the lowest recorded hunter gatherer density of two individuals per 100 km^2 reported for the !Kung (Kelly 1995), and the density of three individuals per 100 km^2 estimated for Middle Paleolithic people (Hassan 1981). However, this discrepancy disappears if humans were restricted to an area some 3–6 times smaller than the entire Sub-Saharan Africa.

Joint Population Analysis and Demographic Assumptions

Our approach to investigate the potential MIS6 bottleneck considered the three African populations separately and do not account for their shared ancestry. Although additional information regarding divergence times, in particular, can be obtained from a joint analysis of the populations, subpopulation-specific analyses are common in modeling studies of population size change and provide robust results regarding the out of Africa bottleneck (Marth et al. 2004; Voight et al. 2005; Li and Durbin 2011). Additionally, the time period of MIS6 is likely more ancient than the divergence of the San population (110–130 kya; Gronau et al. 2011; Veeramah et al. 2012) so that all three populations should be equally affected by demographic changes during MIS6. Using worldwide whole-genome sequence data, Li and Durbin (2011) showed that all African and non-African populations are indeed very similar in their estimated effective population size history before 150 kya. However, because it has been argued that local samples cannot be regarded as being drawn from a panmictic population (Städler et al. 2009), we also considered simulations of a divergence model without a bottleneck where the first divergence involves the San population, and the second one involves the Mandenka and the Biaka populations (Veeramah et al. 2012). We find that there is little variation of the populationwise summary statistics as function of the divergence times (supplementary fig. 5, Supplementary Material online), indicating that using a

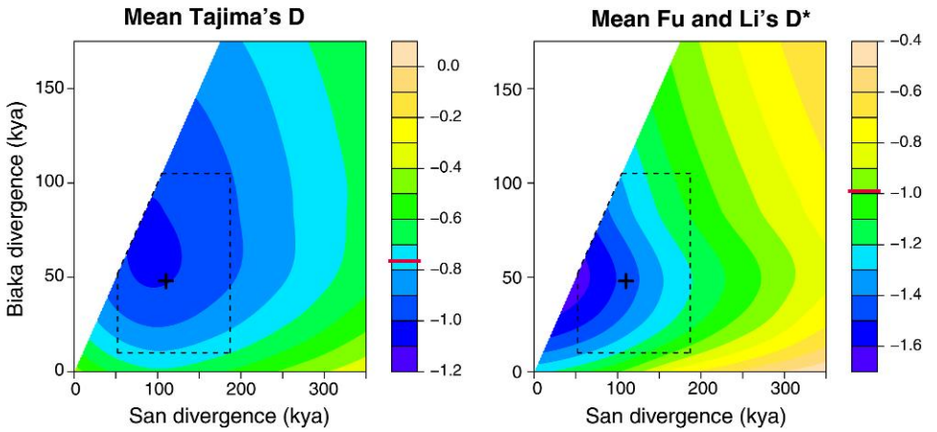

FIG. 6. Mean Tajima's D and Fu and Li's D^* as a function of the Biaka and San divergence times. The summary statistics are computed for a pooled sample containing the Mandenka, San, and Biaka individuals. The cross corresponds to the point estimate provided by Veeramah et al. (2012), and the dashed lines correspond to their 95% credibility intervals. The two horizontal segments correspond to the actual values of $\bar{D} = -0.77$ and $\bar{D}^* = -0.99$ found in the pooled sample. The simulations of the divergence model were performed assuming a constant effective population size of $N = 14,000$ individuals and a mutation rate of $\mu = 2.5 * 10^{-8}$/bp/generation.

divergence model has little practical impact, at least for the summary statistics we considered. Furthermore, when pooling all three populations together, the mean Tajima's D and the mean Fu and Li's D^* decrease (table 1), which can be accounted for by a divergence model (fig. 6). The three populationwise means of Tajima's D are between -0.23 and -0.32 and it decreases to -0.77 when pooling the three populations together. Similarly, the three populationwise means of Fu and Li's D^* are between -0.14 and -0.23 and it decreases to -0.99 for the pooled sample. That these summary statistics decrease with the number of pooled populations is explained by the increase of low-frequency polymorphisms as we pool more and more populations (Ptak and Przeworski 2002; Hammer et al. 2003). Similar to the populationwise analysis, the summary statistics (Tajima's D and Fu and Li's D^*) in the pooled sample can be explained by a demographic model without an ancestral bottleneck.

Another potential limitation of our analysis is the rather crude modeling of population change and there are more general models of piecewise constant trajectories that have been investigated (Minin et al. 2008; Li and Durbin 2011). This being said, accounting for such detail requires more complex models and the fine details of the demographic history will be difficult to detect with genetic data. Providing a fine-scale resolution of demographic history may give the false impression that we can reconstruct extremely detailed fluctuations of population history, but estimates of these fluctuations should not be overinterpreted as some of them may be nonsignificant (see fig. 2 of Li and Durbin 2011).

African Bottlenecks and Population Genetic Data

The fact that African resequencing data are compatible with a demographic model that does not include an ancestral bottleneck confirms previous findings obtained with autosomal sequence data (Pluzhnikov et al. 2002; Adams and Hudson 2004; Voight et al. 2005; Cox et al. 2009; Laval et al. 2010), autosomal SNPs (Marth et al. 2004), and mtDNA (Atkinson et al. 2009). Similarly, a recent analysis found that complete individual genomes from the San, Bantu, and Yoruba populations were consistent with a population expansion in Africa (Gronau et al. 2011). Furthermore, based on two diploid Yoruban genomes, Li and Durbin (2011) found a population expansion during MIS6 confirming the absence of a bottleneck during this time period. However, a peculiarity of their analysis is that the Yoruba population was found to experience a bottleneck that was concomitant with the out-of-Africa bottleneck. Since this result is at odds with most previous results based on resequencing data, additional analyses needs to be performed. There are at least two bottleneck scenarios that would be compatible with the results of Li and Durbin (2011). A worldwide reduction of human population size has been suggested to be a consequence of the eruption of Toba volcano in northern Sumatra some 73,000 years ago (Ambrose 1998; Williams et al. 2009). Another scenario suggests that mega droughts between 75 and 135 kya in East Africa may have promoted population bottlenecks (Scholz et al. 2007). Encouragingly, the pace at which large scale genomic data are accumulating especially from African populations (Tishkoff et al. 2009; Henn et al. 2011) opens the door to a more detailed understanding of human history in the Pleistocene.

Supplementary Material

Supplementary tables 1–6 and figures 1–5 are available at *Molecular Biology and Evolution* online (http://www.mbe.oxfordjournals.org/).

Acknowledgments

This work was supported by a grant from the Swedish Foundation for International Cooperation in Research and Higher Education (STINT) (M.J. and M.B.). M.J. is funded by the Swedish Research Council (2009-5129) and M.B. is funded by the French National Research Agency (DATGEN project, ANR-2010-JCJC-1607-01).

References

Adams AM, Hudson, RR. 2004. Maximum-likelihood estimation of demographic parameters using the frequency spectrum of unlinked single-nucleotide polymorphisms. *Genetics* 168:1699–1712.

Ambrose SH. 1998. Late Pleistocene human population bottlenecks, volcanic winter, and differentiation of modern humans. *J Hum Evol.* 34:623–651.

Amos W, Hoffman JI. 2009. Evidence that two main bottleneck events shaped modern human genetic diversity. *Proc R Soc B.* 277:131–137.

Arora N, Nater A, van Schaik CP, et al. (17 co-authors). 2010. Effects of Pleistocene glaciations and rivers on the population structure of Bornean orangutans (Pongo pygmaeus). *Proc Natl Acad Sci U S A.* 107:21376–21381.

Atkinson QD, Gray RD, Drummond AJ. 2009. Bayesian coalescent inference of major human mitochondrial DNA haplogroup expansions in Africa. *Proc R Soc B.* 276:367–373.

Beaumont MA. 2008. Joint determination of topology, divergence time, and immigration in population trees. In: Matsumura S, Renfrew PFC, editors. Simulation, genetics and human prehistory. Cambridge: McDonald Institute for Archeological Research. p. 134–154.

Beaumont MA, Zhang W, Balding DJ. 2002. Approximate Bayesian computation in population genetics. *Genetics* 162:2025–2035.

Behar DM, Villems R, Soodyall H, et al. (15 co-authors) 2008. The dawn of human matrilineal diversity. *Am J Hum Genet.* 82:1130–1140.

Berlin S, Fogelqvist J, Lascoux M, Lagercrantz U, Rönnberg-Wästljung AC. 2011. Polymorphism and divergence in two willow species, Salix viminalis l. and Salix schwerinii e. wolf. *G3: Genes, Genomes, Genetics* 1:387–400.

Bjork A, Liu W, Wertheim JO, Hahn BH, Worobey M. 2011. Evolutionary history of chimpanzees inferred from complete mitochondrial genomes. *Mol Biol Evol.* 28:615–623.

Blum MGB, François O. 2010. Non-linear regression models for approximate Bayesian computation. *Stat Comput.* 20:63–73.

Blum MGB, Jakobsson M. 2011. Deep divergences of human gene trees and models of human origins. *Mol Biol Evol.* 28:889–898.

Castañeda IS, Mulitza S, Schefuß E, Lopes dos Santos RA, Sinninghe Damsté JS, Schouten S. 2009. Wet phases in the Sahara/Sahel region and human migration patterns in North Africa. *Proc Natl Acad Sci U S A.* 106:20159–20163.

Charlesworth B. 2009. Effective population size and patterns of molecular evolution and variation. *Nat Rev Genet.* 10:195–205.

Cornuet J-M, Ravigne V, Estoup A. 2010. Inference on population history and model checking using DNA sequence and microsatellite data with the software DIYABC (v1.0). *BMC Bioinformatics* 11:401.

Cowling SA, Cox PM, Jones CD, Maslin MA, Peros M, Spall SA. 2008. Simulated glacial and interglacial vegetation across Africa: implications for species phylogenies and trans-African migration of plants and animals. *Glob Change Biol.* 14:827–840.

Cox MP, Morales DA, Woerner AE, Sozanski J, Wall JD, Hammer MF. 2009. Autosomal resequence data reveal late stone age signals of population expansion in sub-saharan african foraging and farming populations. *PLoS One* 4:e6366.

Csilléry K, Blum MGB, Gaggiotti OE, François O. 2010. Approximate Bayesian Computation in practice. *Trends Ecol Evol.* 25:410–418.

Csilléry K, François O, Blum MGB. 2012. abc: an R package for Approximate Bayesian Computation (ABC). *Methods Ecol Evol.* doi:10.1111/j.2041-210X.2011.00179.x.

Depaulis F, Mousset S, Veuille M. 2003. Power of neutrality tests to detect bottlenecks and hitchhiking. *J Mol Evol.* 57:S190–S200.

Dupont LM, Jahns S, Marret F, Ning S. 2000. Vegetation change in equatorial West Africa: time-slices for the last 150 ka. *Palaeogeogr Palaeoclimatol Palaeoecol.* 155:95–122.

Fagundes NJR, Ray N, Beaumont MA, Neuenschwander S, Salzano FM, Bonatto SL, Excoffier L. 2007. Statistical evaluation of alternative models of human evolution. *Proc Natl Acad Sci U S A.* 104:17614–17619.

Frankham R. 1995. Effective population size/adult population size ratios in wildlife: a review. *Genet Res.* 66:95–107.

Galtier N, Depaulis F, Barton N. 2000. Detecting bottlenecks and selective sweeps from DNA sequence polymorphism. *Genetics* 155:981.

Garrigan D, Hammer MF. 2006. Reconstructing human origins in the genomic era. *Nat Rev Genet.* 7:669–680.

Gelman A, Carlin JB, Stern HS, Rubin DB. 2003. Bayesian data analysis. 2nd ed. (Texts in Statistical Science). Boca Raton (FL): Chapman & Hall.

Gonder MK, Mortensen HM, Reed FA, de Sousa A, Tishkoff SA. 2007. Whole-mtDNA genome sequence analysis of ancient African lineages. *Mol. Biol. Evol.* 24:757–768.

Gronau I, Hubisz M, Gulko B, Danko C, Siepel A. 2011. Bayesian inference of ancient human demography from individual genome sequences. *Nat Genet.* 43:1031–1034.

Gutenkunst RN, Hernandez RD, Williamson SH, Bustamante CD. 2009. Inferring the joint demographic history of multiple populations from multidimensional SNP frequency data. *PLoS Genet.* 5:e1000695.

Haddrill PR, Thornton KR, Charlesworth B, Andolfatto P. 2005. Multilocus patterns of nucleotide variability and the demographic and selection history of Drosophila melanogaster populations. *Genome Res.* 15:790–799.

Haffer J. 1969. Speciation in Amazonian forest birds. *Science* 165:131–137.

Hammer MF, Blackmer F, Garrigan D, Nachman MW, Wilder JA. 2003. Human population structure and its effects on sampling Y chromosome sequence variation. *Genetics* 164:1495–1509.

Hammer MF, Woerner AE, Mendez FL, Watkins JC, Cox MP, Wall JD. 2010. The ratio of human X chromosome to autosome diversity is positively correlated with genetic distance from genes. *Nat Genet.* 42:830–831.

Harpending HC, Batzer MA, Gurven M, Jorde LB, Rogers AR, Sherry ST. 1998. Genetic traces of ancient demography. *Proc Natl Acad Sci U S A.* 95:1961–1967.

Hassan F. 1981. Demographic archaeology (Studies in Archaeology). New York: Academic Press.

Hawks J, Hunley K, Lee S-H, Wolpoff M. 2000. Population bottlenecks and Pleistocene human evolution. *Mol Biol Evol.* 17:2–22.

Henn BM, Gignoux CR, Jobin M, et al. (19 co-authors). 2011. Hunter-gatherer genomic diversity suggests a southern African origin for modern humans. *Proc Natl Acad Sci U S A.* 108:5154–5162.

Hetherington R, Reid R. 2010. The climate connection: climate change and modern human evolution. Cambridge: Cambridge University Press.

Hewitt G. 2000. The genetic legacy of the Quaternary ice ages. *Nature* 405:907–913.

Hudson RR. 1987. Estimating the recombination parameter of a finite population model without selection. *Genet Res.* 50:245–250.

Hudson RR. 2002. Generating samples under a Wright-Fisher neutral model of genetic variation. *Bioinformatics* 18:337–338.

Kaessmann H, Wiebe V, Weiss G, Paabo S. 2001. Great ape DNA sequences reveal a reduced diversity and an expansion in humans. *Nat Genet.* 27:155–156.

Kelly RL. 1995. The foraging spectrum: diversity in hunter-gatherer lifeways. Washington (DC): Smithsonian Institution Press.

Klicka J, Zink RM. 1997. The importance of recent ice ages in speciation: a failed paradigm. *Science* 277:1666–1669.

Knight A, Underhill PA, Mortensen HM, Zhivotovsky LA, Lin AA, Henn BM, Louis D, Ruhlen M, Mountain JL. 2003. African Y chromosome and mtDNA divergence provides insight into the history of click languages. *Curr Biol.* 13:464–473.

Lahr MM, Foley RA. 1998. Towards a theory of modern human origins: geography, demography, and diversity in recent human evolution. *Yearb Phys Anthropol.* 107:137–176.

Laval G, Patin E, Barreiro LB, Quintana-Murci L. 2010. Formulating a historical and demographic model of recent human evolution based on resequencing data from noncoding regions. *PLoS One* 5:e10284.

Li H, Durbin R. 2011. Inference of human population history from individual whole-genome sequences. *Nature* 475:493–496.

Lohmueller KE, Bustamante CD, Clark AG. 2010. The effect of recent admixture on inference of ancient human population history. *Genetics* 185:611–622.

Marean CW. 2010. Coastal South Africa and the coevolution of the modern human lineage and the coastal adaptation. In: Bicho N, Haws J, Davis L, editors. Trekking the shore: changing coastlines and the antiquity of coastal settlement. New York: Springer.

Marean CW, Bar-Matthews M, Bernatchez J, et al. (14 co-authors). 2007. Early human use of marine resources and pigment in South Africa during the Middle Pleistocene. *Nature* 499:905–908.

Marth GT, Czabarka E, Murvai J, Sherry ST. 2004. The allele frequency spectrum in genome-wide human variation data reveals signals of differential demographic history in three large world populations. *Genetics* 166:351–372.

McDougall I, Brown FH, Fleagle JG. 2005. Stratigraphic placement and age of modern humans from Kibish, Ethiopia. *Nature* 433:733–736.

Minin VN, Bloomquist EW, Suchard MA. 2008. Smooth skyride through a rough skyline: Bayesian coalescent-based inference of population dynamics. *Mol Biol Evol.* 25:1459–1471.

Nachman MW, Crowell SL. 2000. Estimate of the mutation rate per nucleotide in humans. *Genetics* 156:297–304.

The 1000 Genomes Project Consortium. 2010. A map of human genome variation from population-scale sequencing. *Nature* 467:1061–1073.

Petit J, Jouzel J, Raynaud D, Barkov N, Barnola J, Basile I, Bender M, Chappellaz J, Davis M, Delaygue G. 1999. Climate and atmospheric history of the past 420,000 years from the Vostok ice core, Antarctica. *Nature* 399:429–436.

Plagnol V, Wall JD. 2006. Possible ancestral structure in human populations. *PLoS Genet.* 2:e105.

Pluzhnikov A, Di Rienzo A, Hudson RR. 2002. Inferences about human demography based on multilocus analyses of noncoding sequences. *Genetics* 161:1209–1218.

Pritchard JK, Seielstad MT, Pérez-Lezaun A, Feldman MW. 1999. Population growth of human Y chromosomes: a study of Y chromosome microsatellites. *Mol Biol Evol.* 16:1791–1798.

Pritchard JK, Stephens M, Donnelly P. 2000. Inference of population structure using multilocus genotype data. *Genetics* 155:945–959.

Ptak SE, Przeworski M. 2002. Evidence for population growth in humans is confounded by fine-scale population structure. *Trends Genet.* 18:559–563.

Roach JC, Glusman G, Smit AFA, et al. (15 co-authors). 2010. Analysis of genetic inheritance in a family quartet by whole-genome sequencing. *Science* 328:636–639.

Scholz CA, Johnson TC, Cohen AS, et al. (19 co-authors). 2007. East African megadroughts between 135 and 75 thousand years ago and bearing on early-modern human origins. *Proc Natl Acad Sci U S A.* 104:16416–16421.

Shackleton NJ, Lamb HH, Worssam BC, Hodgson JM, Lord AR, Shotton FW, Schove DJ, Cooper LHN. 1977. The oxygen isotope stratigraphic record of the late pleistocene [and discussion]. *Philos Trans R Soc B.* 280:169–182.

Städler T, Haubold B, Merino C, Stephan W, Pfaffelhuber P. 2009. The impact of sampling schemes on the site frequency spectrum in nonequilibrium subdivided populations. *Genetics* 182: 205–216.

Thornton K. 2003. libsequence: a C++ class library for evolutionary genetic analysis. *Bioinformatics* 19:2325–2327.

Tishkoff SA, Reed FA, Friedlaender FR, et al. (25 co-authors.) 2009. The genetic structure and history of Africans and African Americans. *Science* 324:1035–1044.

Van Andel TH, Tzedakis PC. 1996. Palaeolithic landscapes of Europe and environs, 150,000-25,000 years ago: an overview. *Q Sci Rev.* 15:481–500.

Veeramah KR, Wegmann D, Woerner A, Mendez FL, Watkins JC, Destro-Bisol G, Soodyall H, Louie L, Hammer MF. 2012. An early divergence of KhoeSan ancestors from those of other modern humans is supported by an ABC-based analysis of autosomal resequencing data. *Mol Biol Evol. 29:617–630.*

Voight BF, Adams AM, Frisse LA, Qian Y, Hudson RR, Di Rienzo A. 2005. Interrogating multiple aspects of variation in a full resequencing data set to infer human population size changes. *Proc Natl Acad Sci U S A.* 102:18508–18513.

Wall JD, Cox MP, Mendez FL, Woerner A, Severson T, Hammer MF. 2008. A novel DNA sequence database for analyzing human demographic history. *Genome Res.* 18:1354–1361.

White TD, Asfaw B, DeGusta D, Gilbert H, Richards GD, Suwa G, Clark Howell F. 2003. Pleistocene Homo Sapiens from middle Awash, Ethiopia. *Nature* 423:742–747.

Williams MAJ, Ambrose SH, van der Kaars S, Ruehlemann C, Chattopadhyaya U, Pal J, Chauhan PR. 2009. Environmental impact of the 73 ka Toba super-eruption in South Asia. *Palaeogeogr Palaeoclimatol Palaeoecol.* 284:295–314.